Cancer Research

Antineoplastic Mechanisms of Niclosamide in Acute Myelogenous Leukemia Stem Cells: Inactivation of the NF-κB Pathway and Generation of Reactive Oxygen Species

Yanli Jin[1], Zhongzheng Lu[1], Ke Ding[2], Juan Li[3], Xin Du[4], Chun Chen[5], Xiaoyong Sun[1], Yongbin Wu[1], Jing Zhou[2], and Jingxuan Pan[1]

Abstract

NF-κB may be a potential therapeutic target for acute myelogenous leukemia (AML) because NF-κB activation is found in primitive human AML blast cells. In this report, we initially discovered that the potent antineoplastic effect of niclosamide, a Food and Drug Administration–approved antihelminthic agent, was through inhibition of the NF-κB pathway in AML cells. Niclosamide inhibited the transcription and DNA binding of NF-κB. It blocked tumor necrosis factor–induced IκBα phosphorylation, translocation of p65, and expression of NF-κB–regulated genes. Niclosamide inhibited the steps TAK1→IκB kinase (IKK) and IKK→IκBα. Niclosamide also increased the levels of reactive oxygen species (ROS) in AML cells. Quenching ROS by the glutathione precursor *N*-acetylcysteine attenuated niclosamide-induced apoptosis. Our results together suggest that niclosamide inhibited the NF-κB pathway and increased ROS levels to induce apoptosis in AML cells. On translational study of the efficacy of niclosamide against AML, niclosamide killed progenitor/stem cells from AML patients but spared those from normal bone marrow. Niclosamide was synergistic with the frontline chemotherapeutic agents cytarabine, etoposide, and daunorubicin. It potently inhibited the growth of AML cells *in vitro* and in nude mice. Our results support further investigation of niclosamide in clinical trials of AML patients. *Cancer Res; 70(6); 2516–27. ©2010 AACR.*

Introduction

Acute myelogenous leukemia (AML) is a major type of hematologic malignancy. Chemotherapy remains an important therapeutic approach. However, in the past 3 decades, limited progress has been achieved in improving the long-term disease-free survival, except for certain subtypes of AML (e.g., acute promyelocytic leukemia). Cytarabine (Ara-C), etoposide (VP-16), and daunorubicin (DNR) remain frontline agents (1). Therefore, the development of innovative therapies and identification of more effective drugs for AML has high priority.

Recently, interest has increased in molecularly targeted therapy for AML. The development of tyrosine kinase inhibitors [e.g., PKC412 (2) and sorafenib (3)] brought promise for the subtype of AML patients with activating mutations of Flt3 [e.g., Flt3 internal tandem duplication (Flt3-ITD)]. However, ~50% of AML patients have normal karyotypes. Accordingly, the selection of molecular targets for therapeutic intervention is not obvious for these AML cases.

NF-κB plays a critical role in inflammation, antiapoptotic responses, and carcinogenesis (4–7). High NF-κB expression is found in primitive human AML blast cells (8–11). In particular, the constitutive activation of NF-κB exists selectively in leukemia stem cells but not in normal hematopoietic stem cells (11). Therefore, NF-κB may be a potential therapeutic target for the selective eradication of leukemia stem cells. Indeed, pharmacologic inhibition of NF-κB was effective in killing AML cells (12, 13).

In this report, we validated the inhibitory action of niclosamide against tumor necrosis factor (TNF)–induced NF-κB activation in AML cells and identified its mechanism, together with generation of reactive oxygen species (ROS), as being responsible for induced apoptosis of AML cells. We also report on our translational studies showing the synergism of niclosamide with frontline chemotherapeutic agents for AML, the presence of a therapeutic window, and the *in vivo* antineoplastic efficacy in a mouse model.

Materials and Methods

Chemicals and Antibodies

Niclosamide (2′,5-dichloro-4′-nitrosalicylanilide), *N*-acetylcysteine (NAC), Ara-C, DNR, VP-16, Annexin V–FITC, and anti-actin were from Sigma-Aldrich. A water-soluble derivative

Authors' Affiliations: [1]Department of Pathophysiology, Zhongshan School of Medicine, Sun Yat-sen University; [2]Key Laboratory of Regenerative Biology and Institute of Chemical Biology, Guangzhou Institute of Biomedicine and Health, Chinese Academy of Sciences; [3]Department of Hematology, The First Affiliated Hospital, Sun Yat-sen University; [4]Department of Hematology, Guangdong Provincial People's Hospital; [5]Department of Pediatrics, Sun Yat-sen Memorial Hospital, Sun Yat-sen University, Guangzhou, China

Note: Supplementary data for this article are available at Cancer Research Online (http://cancerres.aacrjournals.org/).

Corresponding Author: Jingxuan Pan, Department of Pathophysiology, Zhongshan School of Medicine, Sun Yat-sen University, 74 Zhongshan Road II, Guangzhou 510089, China. Phone/Fax: 86-20-8733-2788; E-mail: panjx2@mail.sysu.edu.cn.

doi: 10.1158/0008-5472.CAN-09-3950

of niclosamide, designated *p*-niclosamide, was obtained by the addition of a phosphate group to niclosamide with diethyl phosphite. CM-H_2DCF-DA was from Invitrogen. Niclosamide was dissolved in DMSO at a stock concentration of 10 mmol/L and stored at −20°C. Recombinant human TNFα was from PeproTech. Antibodies against p65, IκBα, proliferating cell nuclear antigen (PCNA), cyclin D1, Bcl-X_L, and Mcl-1 were from Santa Cruz Biotechnology. Antibodies against poly(ADP-ribose) polymerase (PARP), caspase-3, X-linked inhibitor of apoptosis protein (XIAP), cytochrome *c*, CD34-FITC, and CD38-phycoerythrin (PE) were from BD Biosciences. Antibodies against c-myc, phospho-IKKα (S180)/IKKβ (S181), phospho-IκBα (S32), phospho-p65 (S536), phospho–extracellular signal-regulated kinase 1/2 (ERK1/2; T202/Y204), ERK1/2, phospho-AKT (S473), AKT, phospho-p38 (T180/Y182), p38, phospho–c-Jun NH_2-terminal kinase (JNK; T183/Y185), and JNK were from Cell Signaling Technology. Anti-IKKβ and anti-Bim were from Upstate Technology. Anti-survivin was from Novus Biologicals.

Cell Culture

HL-60, U937, OCI-AML3, Molm13, MV4-11, and U266 cells were grown in RPMI 1640 (Invitrogen) with 10% FCS (Biological Industries). The mitochondrial respiration-deficient ρ^- cells (C6F/HL-60) were established and cultured as described (14). U2OS cells, mouse embryonic fibroblast (MEF), and normal human fibroblast (NHFB) cell lines were cultured in DMEM supplemented with 10% FCS (15, 16).

Primary Cells from AML Patients

Peripheral blood or bone marrow samples were obtained from patients with AML (68 cases), acute lymphoblastic leukemia (ALL; 10 cases), or chronic myelogenous leukemia (CML; 3 cases) and from 7 healthy adult donors in The First Affiliated Hospital, Sun Yat-sen Memorial Hospital of Sun Yat-sen University, and Guangdong Provincial People's Hospital after patients gave their informed consent. The study followed institutional guidelines and the Declaration of Helsinki principles. The clinical information for the 81 patients is in Supplementary Table S1.

Preparation of Whole-Cell Lysates and Cytosolic Fraction

Whole lysates were prepared with radioimmunoprecipitation assay buffer (16, 17). The cytosolic fraction was prepared with digitonin extraction buffer to detect the level of cytochrome *c* in the cytosol, as described previously (16, 17).

Preparation of Cytoplasmic and Nuclear Fractions

Cytoplasmic and nuclear fractions were prepared as described previously (18).

Luciferase Assay

U2OS cells were transfected with reporter plasmids encoding NF-κB–TATA-Luc (0.5 μg) and pEF*Renilla*-Luc (10 ng) or together with plasmids encoding the desired genes by use of Lipofectamine 2000 (Invitrogen). Luciferase activities were measured with use of dual-luciferase assay kits (Promega) as described (19). NF-κB activities were determined by normalizing the activity of NF-κB–dependent firefly luciferase to that of *Renilla* luciferase. The pNF-κB-Luc plasmid was from Stratagene. The plasmids pCMV5-IKKα, pCMV5-IKKβ, pCMV5-IKKγ, pCMV5-p65, and pCMV5-myc-TAK1 used for cotransfection experiments were described (20, 21).

Electrophoretic Mobility Shift Assay

Electrophoretic mobility shift assay (EMSA) involved use of the LightShift Chemiluminescent EMSA kit (Pierce Biotechnology) according to the manufacturer's instructions (22). The oligonucleotides for NF-κB were from Promega: forward, 5′-AGTTGAGGGGACTTTCCCAGGC-3′; reverse, 5′-GCCTGGGAAAGTCCCCTCAACT-3′.

Immunofluorescence Staining

Immunofluorescence staining was as described previously (17, 23).

Cell Viability Assay

Cell viability was determined by MTS assay (CellTiter 96 Aqueous One Solution Cell Proliferation assay, Promega; refs. 15, 16). The drug concentration resulting in 50% inhibition of cell growth (IC_{50}) was determined.

Flow Cytometry

Measurement of apoptosis and mitochondrial transmembrane potential, as well as analysis of cell cycle and intracellular ROS levels, was as described (16, 17, 24).

Colony-Forming Assays

Soft agar clonogenic assay in AML cell lines. AML cell lines were treated with niclosamide or diluent (DMSO, control) for 24 h, then washed with PBS, and seeded in Iscove's medium containing 0.3% agar and 20% FCS in the absence of drug treatment (16).

Colony-forming assay in normal bone marrow cells and primary AML blast cells. The colony-forming capacity of normal bone marrow cells and primary AML blast cells was analyzed by use of methylcellulose medium (Methocult H4434, Stem Cell Technologies) according to the manufacturer's instructions. Niclosamide was added to the initial cultures at 0.1 to 10 μmol/L. After 14 d of culture, the number of colony-forming units (CFU) was evaluated under an inverted microscope according to the standard criteria (25).

Tumor Xenograft Experiments

Male *nu/nu* BALB/c mice were bred at the animal facility of Sun Yat-sen University. HL-60 cells were inoculated s.c. on the flanks of 4- to 6-wk-old mice. Tumors were measured every other day with use of calipers. Tumor volumes were calculated by the following formula: $a^2 \times b \times 0.4$, where a is the smallest diameter and b is the diameter perpendicular to a. After mice were euthanized, xenografts were dissected, weighed, or preserved. All animal studies were approved by the Sun Yat-sen University Institutional Animal Care and Use Committee.

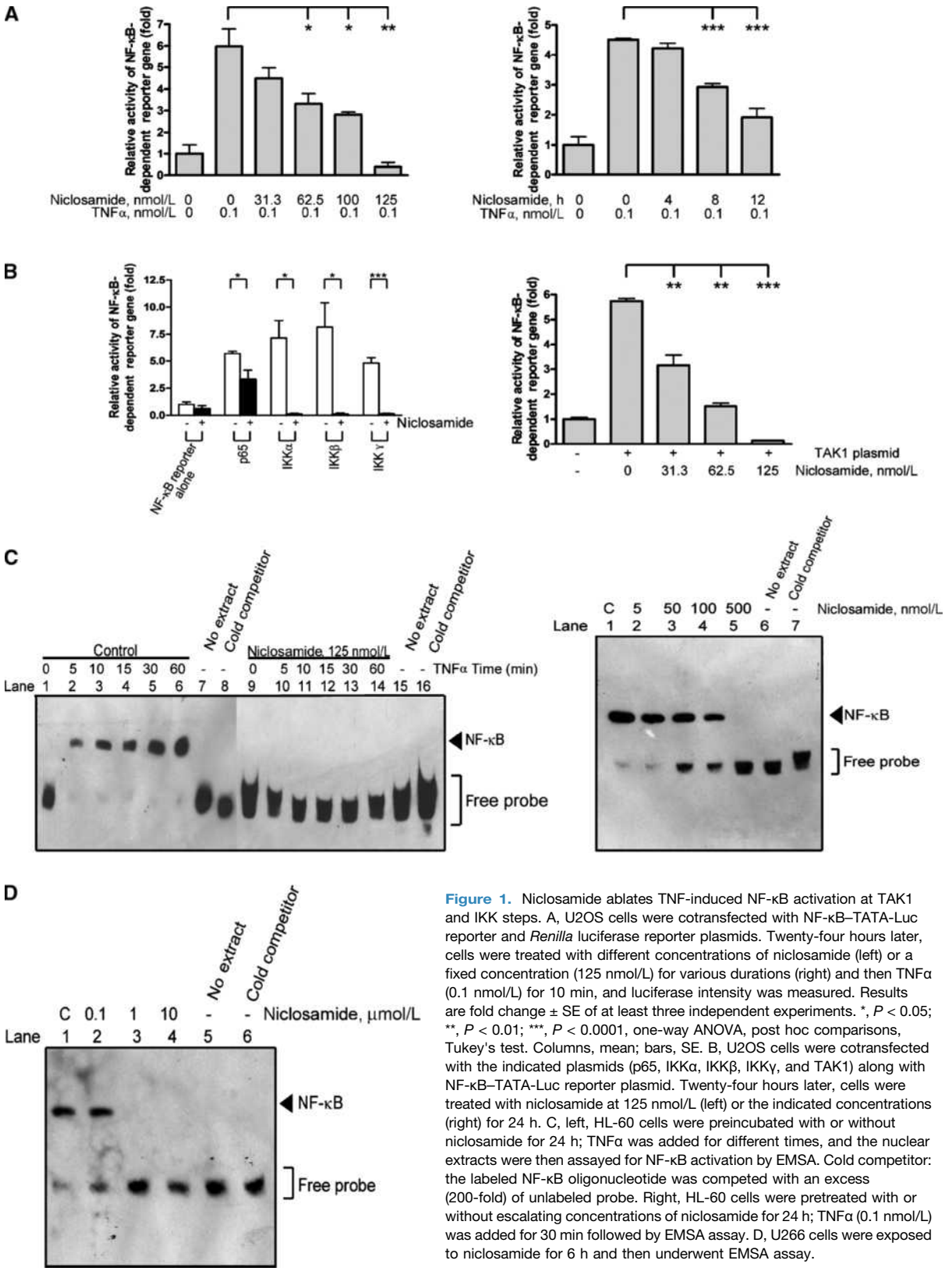

Figure 1. Niclosamide ablates TNF-induced NF-κB activation at TAK1 and IKK steps. A, U2OS cells were cotransfected with NF-κB–TATA-Luc reporter and *Renilla* luciferase reporter plasmids. Twenty-four hours later, cells were treated with different concentrations of niclosamide (left) or a fixed concentration (125 nmol/L) for various durations (right) and then TNFα (0.1 nmol/L) for 10 min, and luciferase intensity was measured. Results are fold change ± SE of at least three independent experiments. *, $P < 0.05$; **, $P < 0.01$; ***, $P < 0.0001$, one-way ANOVA, post hoc comparisons, Tukey's test. Columns, mean; bars, SE. B, U2OS cells were cotransfected with the indicated plasmids (p65, IKKα, IKKβ, IKKγ, and TAK1) along with NF-κB–TATA-Luc reporter plasmid. Twenty-four hours later, cells were treated with niclosamide at 125 nmol/L (left) or the indicated concentrations (right) for 24 h. C, left, HL-60 cells were preincubated with or without niclosamide for 24 h; TNFα was added for different times, and the nuclear extracts were then assayed for NF-κB activation by EMSA. Cold competitor: the labeled NF-κB oligonucleotide was competed with an excess (200-fold) of unlabeled probe. Right, HL-60 cells were pretreated with or without escalating concentrations of niclosamide for 24 h; TNFα (0.1 nmol/L) was added for 30 min followed by EMSA assay. D, U266 cells were exposed to niclosamide for 6 h and then underwent EMSA assay.

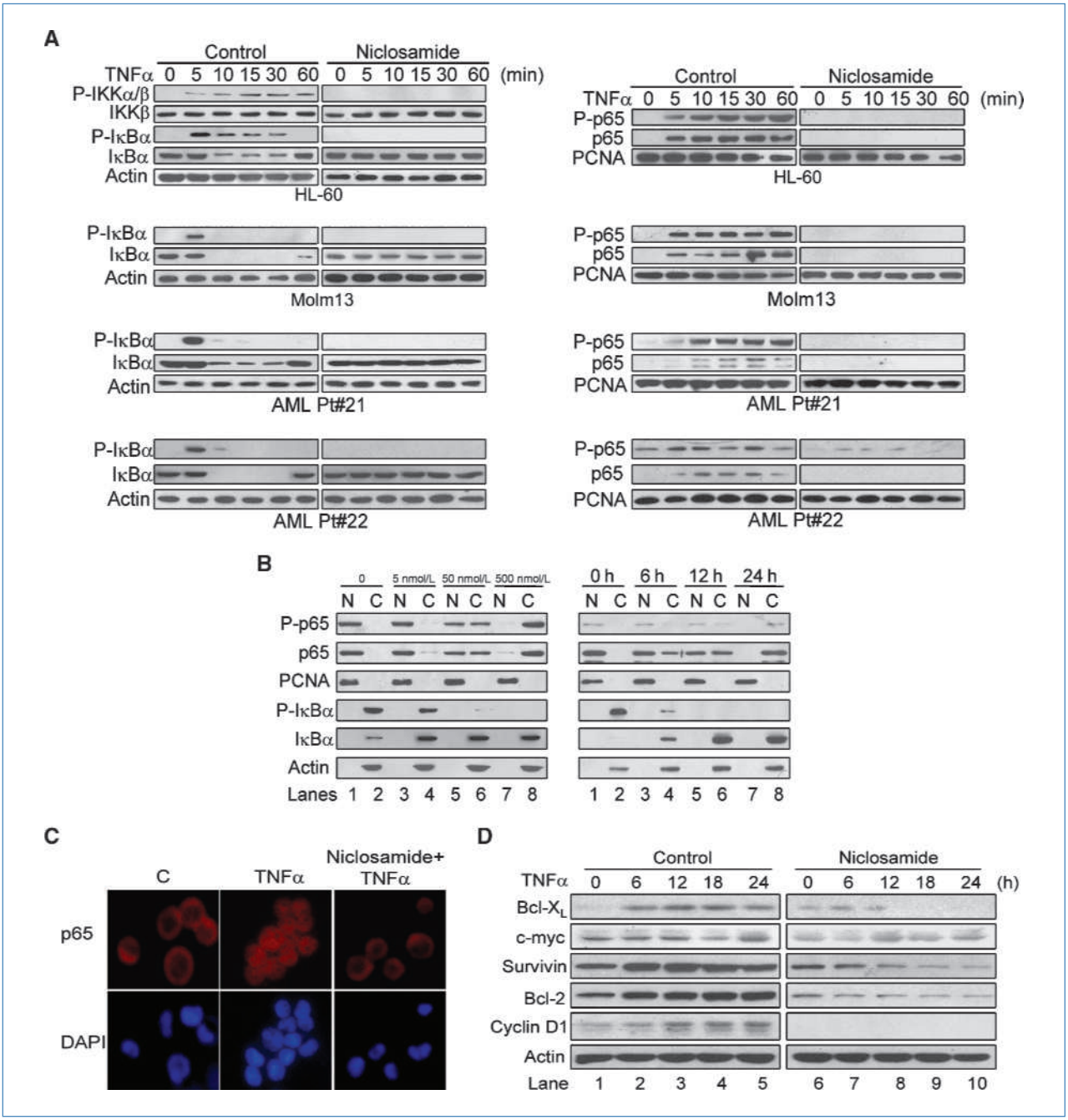

Figure 2. Niclosamide inhibits TNF-induced degradation of IκBα and relocation of p65. A, HL-60, Molm13, or AML primary cells were preincubated with 500 nmol/L niclosamide for 24 h and then treated with TNFα (0.1 nmol/L) for the indicated times; cytoplasmic (left) and nuclear (right) extracts were examined by immunoblotting. Actin and PCNA served as markers of cytoplasmic and nuclear extractions, respectively. B, dose- and time-dependent effect of niclosamide. HL-60 cells were pretreated with the indicated concentrations of niclosamide for 24 h (left) or 500 nmol/L niclosamide for various durations; cytoplasmic (C) and nuclear (N) extracts were examined by immunoblotting. C, immunofluorescence staining analysis of p65 localization. HL-60 cells were preincubated with 500 nmol/L niclosamide for 24 h and TNFα (1 nmol/L) for 15 min, fixed, and then underwent immunofluorescence analysis. Nuclei were stained with 4′,6-diamidino-2-phenylindole (DAPI). D, niclosamide represses the expression of NF-κB–regulated proteins involved in cell survival. Western blot analysis of HL-60 cells pretreated with 500 nmol/L niclosamide for 24 h and then stimulated with TNFα (1 nmol/L) for different times.

Measurement of Apoptosis in Progenitor/Stem Cells

Bone marrow mononuclear cells from AML patients and normal healthy donors were isolated by immunomagnetic separation by use of CD34 selection MACS kits (Miltenyi Biotec) according to the manufacturer's protocol. The magnetically labeled CD34$^+$ cells recovered from the column were cultured in Iscove's modified Dulbecco's medium supplemented with appropriate cytokines (PeproTech). An aliquot

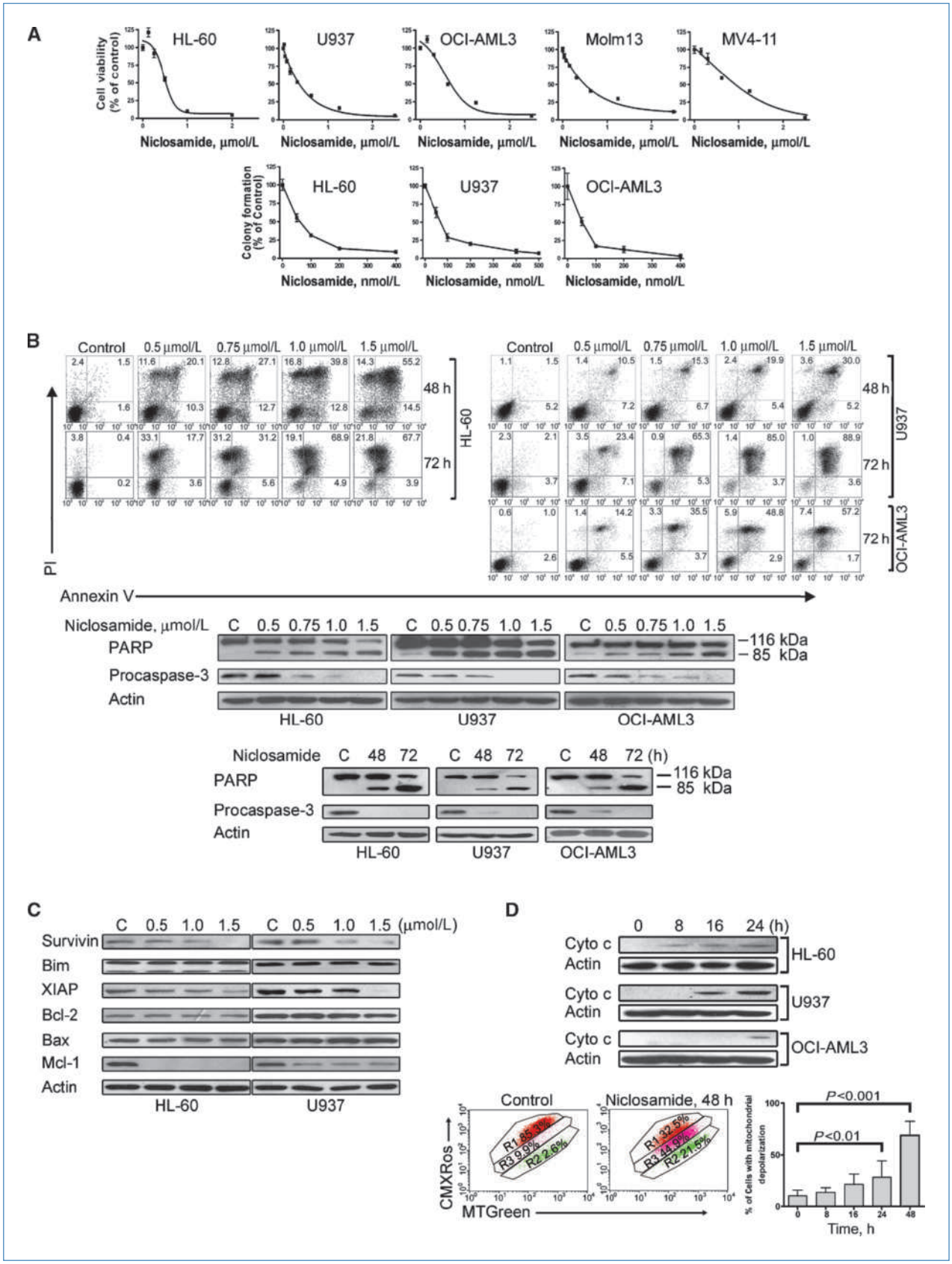
A
Cell viability (% of control)
HL-60
U937
OCI-AML3
Molm13
MV4-11
Niclosamide, μmol/L
Colony formation (% of Control)
Niclosamide, nmol/L
B
Control
0.5 μmol/L
0.75 μmol/L
1.0 μmol/L
1.5 μmol/L
48 h
72 h
HL-60
U937
OCI-AML3
PI
Annexin V
Niclosamide, μmol/L
PARP
Procaspase-3
Actin
116 kDa
85 kDa
Niclosamide
48
72 (h)
C
Survivin
Bim
XIAP
Bcl-2
Bax
Mcl-1
(μmol/L)
D
0
8
16
24 (h)
Cyto c
Actin
Control
Niclosamide, 48 h
CMXRos
MTGreen
R1 85.3%
R3 9.9%
R2 2.6%
R1 32.5%
R3 44.9%
R2 21.5%
% of Cells with mitochondrial depolarization
P<0.001
P<0.01
Time, h

underwent flow cytometry after CD34-FITC staining. The rest of the cells were cultured with or without niclosamide for 24 h. The cells were then analyzed by flow cytometry after staining with CD38-PE and Annexin V–FITC. The Annexin $V^+CD34^+CD38^-$ subpopulation was compared.

Statistical Analysis

All experiments were performed at least thrice, and results are expressed as the mean ± SE, unless otherwise stated. GraphPad Prism 4.0 software (GraphPad Software) was used for statistical analysis. A P value of <0.05 was considered statistically significant.

Results

Niclosamide inhibits TNF-induced NF-κB–dependent reporter gene transcription. We first examined whether niclosamide affected the TNF-induced NF-κB–dependent reporter gene transcription. U2OS cells were cotransfected with pNF-κB–TATA-Luc and pEF*Renilla*-Luc for 24 hours and then treated with niclosamide. After stimulation with TNFα, the luciferase activity increased, but niclosamide inhibited the TNF-induced NF-κB reporter activity in a dose- and time-dependent manner (Fig. 1A).

Niclosamide inhibits NF-κB activation induced by p65, IKKα, IKKβ, IKKγ, and TAK1. Cotransfection of p65, IKKα, IKKβ, IKKγ, or TAK1 constructs markedly increased the luciferase activity of NF-κB–TATA-Luc reporter; niclosamide significantly abrogated this increase (Fig. 1B). Therefore, niclosamide could block the IKK- or TAK1-induced NF-κB activation. Considering the critical role of TAK1 in TNF-induced activation of IKK (26), and niclosamide inhibiting TNF-induced IKK phosphorylation (Fig. 2A), niclosamide may exert its inhibitory effect at the TAK1 step (model in Fig. 4D, right).

Niclosamide inhibits DNA binding of NF-κB. We next determined whether niclosamide affected the binding of NF-κB to DNA by EMSA. The levels of the NF-κB–DNA complex were steadily increased on TNFα stimulation (Fig. 1C, left). The TNF-induced bound complex disappeared when the labeled NF-κB oligonucleotide competed with an excess (200-fold) of unlabeled probe (Fig. 1C, left), indicating the binding specificity of this assay. Pretreatment with niclosamide completely blocked the time- and dose-dependent TNFα-induced alteration of the NF-κB–DNA complex (Fig. 1C).

Niclosamide inhibits constitutive NF-κB activation. Because constitutive activation of NF-κB exists in certain tumor cells such as multiple myeloma U266 cells (18), we tested and found that niclosamide inhibited constitutively active NF-κB binding to DNA in U266 cells (Fig. 1D).

Niclosamide inhibits TNF-induced degradation of IκBα and relocation of p65 in a dose- and time-dependent manner. Immunoblotting showed that in the absence of niclosamide (Fig. 2A, left, top), the levels of phosphorylated IKKα/β and phosphorylated IκBα steadily increased in HL-60 cells beginning at 5 minutes after TNFα stimulation. Concomitantly, the levels of total IκBα progressively decreased, which was consistent with phosphorylation of IκBα activating ubiquitination and degradation (5). In contrast, niclosamide completely abolished the TNFα-induced phosphorylation of IKKα/β and IκBα (Fig. 2A, left, top). Accordingly, the TNFα-induced degradation of IκBα was abrogated by niclosamide. Conversely, the levels of phosphorylated and total p65 in the nuclear fractions were increased in TNF-stimulated cells, but niclosamide abrogated the TNF-induced nuclear translocation of p65 (Fig. 2A, right, top). Similar findings were obtained in Molm13 cells and primary AML blast cells (Fig. 2A). Niclosamide abrogating NF-κB activation in HL-60 cells was dose and time dependent (Fig. 2B). This potent inhibitory activity was confirmed in 12 of 12 additional AML patients (Supplementary Fig. S1). The inhibitory effect of niclosamide on TNF-induced translocation of p65 was further confirmed by immunofluorescent microscopy (Fig. 2C).

Niclosamide decreases TNF-induced NF-κB–dependent gene products involved in cell survival. HL-60 cells were pretreated with or without niclosamide for ~24 hours and then stimulated with TNFα; the levels of Bcl-X_L, c-myc, survivin, Bcl-2, and cyclin D1 were increased (Fig. 2D, left), and the TNF-induced upregulation was abolished by niclosamide (Fig. 2D, right).

Because TNFα activates multiple pathways, we examined the selective activity of niclosamide. Niclosamide inhibited the TNF-induced activation of AKT, which is upstream of TAK1 (27), but not ERK1/2, JNK, or p38 (Supplementary Fig. S2).

Niclosamide inhibits growth of AML cell lines **in vitro.** We evaluated the activity of niclosamide in AML cells by MTS. Niclosamide dose dependently inhibited the growth of AML cells within the nanomolar range (Fig. 3A, top).

We also measured the effect of niclosamide on anchorage-independent growth of AML cells in soft agar culture. Niclosamide dose dependently inhibited the number of surviving clonogenic AML cells, with IC_{50} values of 69.5 to 95 nmol/L (Fig. 3A, bottom).

Niclosamide induces apoptosis in AML cells. Niclosamide induced robust apoptosis as detected by flow cytometry after Annexin V–FITC/PI staining in AML cells (Fig. 3B). It

Figure 3. Niclosamide induces apoptosis in AML cells by triggering an intrinsic pathway. A, top, cell viability was measured by MTS assay in five lines of AML cells after 72-h treatment with niclosamide; bottom, clonogenicity of AML cells in soft agar was inhibited by niclosamide in a dose-dependent manner. B, HL-60 cells were exposed to niclosamide. Top, apoptosis was evaluated on flow cytometry; middle and bottom, dose- and time-dependent change in PARP and procaspase-3 detected by immunoblotting. C, immunoblotting of apoptosis-related proteins in AML cells after 48-h treatment with niclosamide. D, top, niclosamide led to release of cytochrome *c* into cytosol in AML cells. Levels of cytochrome *c* in the cytosolic extracts prepared with digitonin buffer were detected by immunoblotting. Bottom, HL-60 cells treated with or without niclosamide were stained with CMXRos and MTGreen, and mitochondrial potential was analyzed by flow cytometry. Left, representative fluorescent histograms from three independent experiments; right, vertical axis represents the sum of R2 and R3.

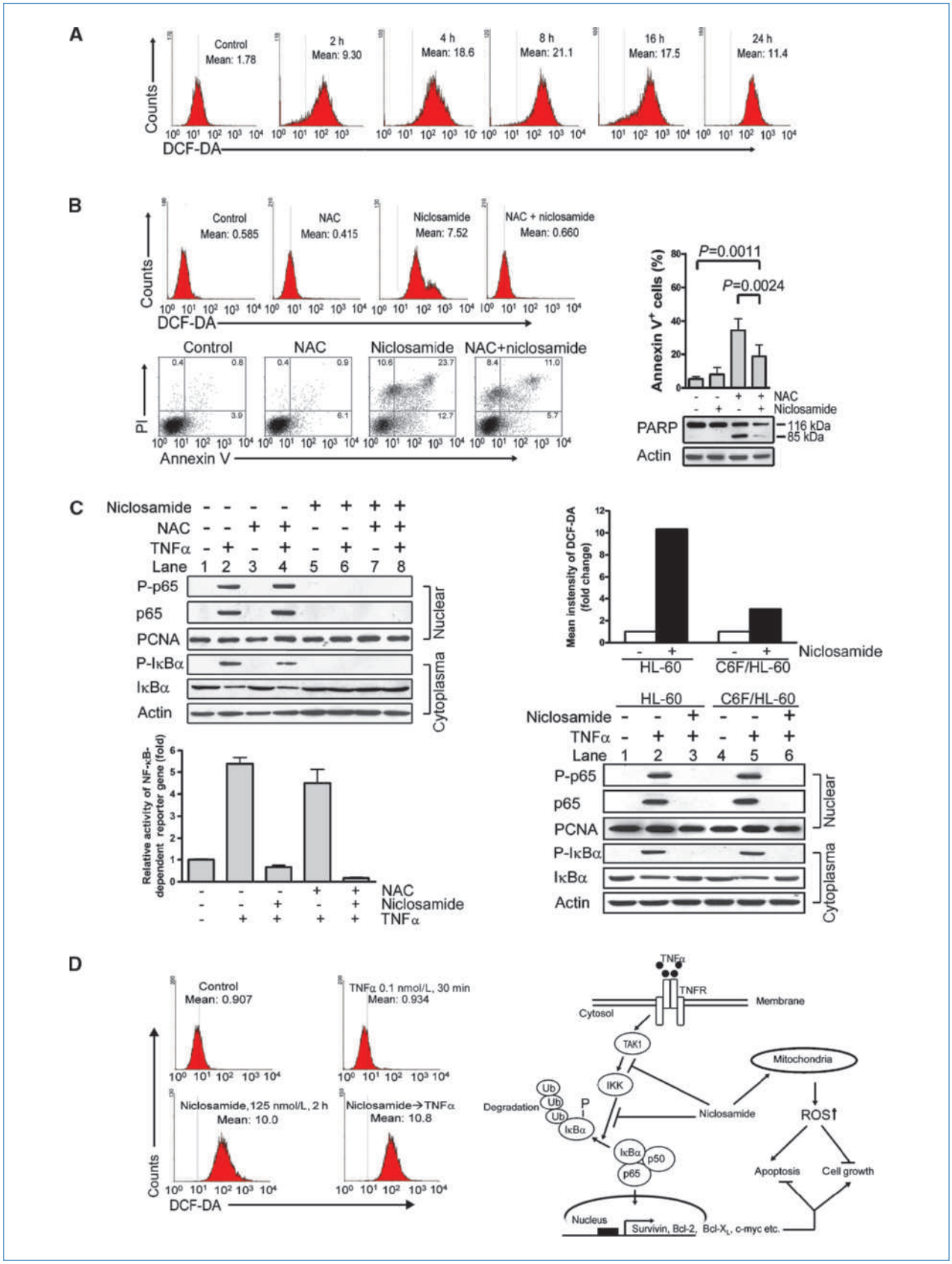
A
Control
Mean: 1.78
2 h
Mean: 9.30
4 h
Mean: 18.6
8 h
Mean: 21.1
16 h
Mean: 17.5
24 h
Mean: 11.4
Counts
DCF-DA
B
Control
Mean: 0.585
NAC
Mean: 0.415
Niclosamide
Mean: 7.52
NAC + niclosamide
Mean: 0.660
Counts
DCF-DA
Control
NAC
Niclosamide
NAC+niclosamide
PI
Annexin V
Annexin V+ cells (%)
P=0.0011
P=0.0024
NAC
Niclosamide
PARP
116 kDa
85 kDa
Actin
C
Niclosamide
NAC
TNFα
Lane 1 2 3 4 5 6 7 8
P-p65
p65
PCNA
P-IκBα
IκBα
Actin
Nuclear
Cytoplasma
Relative activity of NF-κB-dependent reporter gene (fold)
NAC
Niclosamide
TNFα
Mean instensity of DCF-DA (fold change)
HL-60
C6F/HL-60
Niclosamide
HL-60
C6F/HL-60
Niclosamide
TNFα
Lane 1 2 3 4 5 6
P-p65
p65
PCNA
P-IκBα
IκBα
Actin
Nuclear
Cytoplasma
D
Control
Mean: 0.907
TNFα 0.1 nmol/L, 30 min
Mean: 0.934
Niclosamide, 125 nmol/L, 2 h
Mean: 10.0
Niclosamide→TNFα
Mean: 10.8
Counts
DCF-DA
TNFα
TNFR
Membrane
Cytosol
TAK1
IKK
Mitochondria
Ub
Degradation
P
IκBα
Niclosamide
ROS↑
IκBα
p50
p65
Apoptosis
Cell growth
Nucleus
Survivin, Bcl-2, Bcl-XL, c-myc etc.

induced a dose- and time-dependent specific cleavage of PARP and a decrease in the precursor form of caspase-3, further indicating onset of apoptosis (Fig. 3B, bottom two panels).

Niclosamide decreases Mcl-1 and XIAP levels and leads to mitochondrial damage. Niclosamide led to decreased levels of Mcl-1 and XIAP in AML cells (Fig. 3C) and elevated levels of cytochrome *c* in the cytosolic fractions and to mitochondrial depolarization in HL-60 cells (Fig. 3D). Therefore, niclosamide triggered the intrinsic apoptosis pathway.

Niclosamide does not affect cell cycling. Niclosamide had a minimal effect on cell cycling in AML cells, except for the appearance of the sub-G_1 apoptotic population (Supplementary Fig. S3).

Niclosamide generates ROS in AML cells. Niclosamide was reported to inhibit the NADH→$NADP^+$ transhydrogenation on *Hymenolepis diminuta* submitochondrial particle assay (28, 29). We therefore assessed whether niclosamide induced intracellular ROS generation. Niclosamide increased intracellular ROS levels in HL-60 cells at 2 hours, which peaked at 8 hours (Fig. 4A).

Niclosamide-induced ROS elevation partially contributes to apoptosis of AML cells. Because ROS generation is an important mechanism for certain chemotherapeutic agents to kill tumor cells (30), we next examined whether the niclosamide-induced ROS elevation facilitated its cytotoxicity in AML cells. Although NAC completely blocked the niclosamide-induced ROS elevation (Fig. 4B, left, top), quenching ROS by NAC attenuated but did not completely abrogate niclosamide-mediated apoptosis, which was reflected by Annexin V–positive cell population and PARP cleavage (Fig. 4B). Therefore, ROS elevation partially contributed to the cytotoxicity of niclosamide and may be a mechanism parallel to NF-κB inhibition.

ROS elevation and NF-κB inactivation are independent mechanisms of niclosamide. Redox regulation of NF-κB is controversial: ROS can activate or inhibit NF-κB (31, 32). By using the dual activities of niclosamide, we examined whether TNF-induced NF-κB activation was regulated by ROS. NAC did not prevent the TNF-induced phosphorylation or degradation of IκBα or translocation of p65 (Fig. 4C, left, top). However, in the presence of NAC, niclosamide completely blocked TNF-induced IκBα phosphorylation and p65 translocation.

We next addressed whether ROS played a role in TNF-induced NF-κB–dependent reporter gene transcription. Quenching ROS by NAC did not substantially attenuate the TNF-induced elevation of NF-κB transcription activity (Fig. 4C, left, bottom). In the presence of NAC, niclosamide completely abrogated the TNF-induced elevation of NF-κB transcription.

The mitochondrial respiration-deficient ρ^- cells were used to further ascertain whether ROS affected the TNFα-induced NF-κB activation. We hypothesized that ρ^- cells generated less ROS in response to niclosamide treatment because of their deficient mitochondrial aerobic respiration. After niclosamide treatment, mean intracellular ROS level was increased ~10-fold in parental HL-60 cells but only 3-fold in ρ^- cells (Fig. 4C, right, top). We next compared the TNF-induced NF-κB activation in this pair of cells. Parental HL-60 cells and ρ^- cells were pretreated with or without niclosamide, and then TNFα was added in the culture. Immunoblotting revealed that IκBα phosphorylation and p65 translocation occurred to the same extent in parental HL-60 cells as in ρ^- cells (Fig. 4C, right, bottom). Therefore, niclosamide inhibited the TNFα-induced NF-κB activation in a ROS-independent manner.

Conversely, we determined whether TNF-induced NF-κB activation affected ROS generation. Because marked repression of NF-κB by niclosamide requires >4 hours of incubation with niclosamide (Fig. 1A, right), we chose 2-hour niclosamide treatment to induce a significant elevation of ROS with minimal effect on NF-κB activation. After HL-60 cells were exposed to 125 nmol/L niclosamide for 1.5 hours, cells were stimulated with TNFα, and then ROS level was detected. TNFα did not influence the niclosamide-induced ROS generation (Fig. 4D, left).

Niclosamide is synergistic with Ara-C, VP-16, and DNR. Because of the high potency of niclosamide in AML cells, we assessed its effect on normal cells. MEF, NHFB cells, and bone marrow cells from four healthy individuals were treated with niclosamide for 72 hours; cell viability assay revealed niclosamide with minimal effects on growth of these normal cells (Supplementary Table S2). Therefore, the differential sensitivity of niclosamide in AML cells and normal cells implies a therapeutic window for niclosamide.

We next examined a synergism between niclosamide and the frontline chemotherapeutic agents for AML (e.g., Ara-C, VP-16, and DNR) in causing growth inhibition. HL-60 and U937 cells were incubated in a serially diluted mixture (at a fixed ratio) of niclosamide and Ara-C, VP-16, or DNR for 72 hours and then underwent MTS assay. Synergism was evaluated by the median-effect method of Chou and Talalay (16). Niclosamide and all three drugs synergistically [i.e., combination index (CI) < 1] inhibited viability of AML cells (Fig. 5A).

Given that Molm13 cells bearing Flt3-ITD were also sensitive to niclosamide (Fig. 3A), we examined a synergistic effect

Figure 4. Niclosamide elevates ROS in AML cells. A, HL-60 cells were exposed to niclosamide for various times, and then ROS was detected by flow cytometry after staining with 2.5 μmol/L CM-H_2DCF-DA. The dotted line indicates the mean intensity in control cells. The mean intensity of DCF-DA is shown. B, HL-60 cells were preincubated with 2 mmol/L NAC for 1 h before being exposed to 500 nmol/L niclosamide for 36 h. Cells underwent flow cytometry for ROS or apoptosis and immunoblotting (n = 3). C, left, top, immunoblotting of HL-60 cells exposed to 500 nmol/L niclosamide for 24 h with or without 2 mmol/L NAC; TNFα (0.1 nmol/L) was then added for 30 min. Bottom, U2OS cells were transfected with NF-κB–TATA-Luc reporter plasmid. Twenty-four hours later, cells were treated with 125 nmol/L niclosamide for another 24 h with or without 2 mmol/L NAC. The luciferase activity was assayed after 30-min stimulation with TNFα (0.1 nmol/L). Right, top, intracellular ROS content in parental HL-60 cells versus ρ^- (C6F/HL-60) cells after 24-h treatment with or without 500 nmol/L niclosamide; bottom, immunoblotting of IκBα and p65 in parental HL-60 cells versus ρ^- cells. D, left, ROS analysis in HL-60 cells after treatment with niclosamide and TNFα; right, a proposed model to delineate the actions of niclosamide.

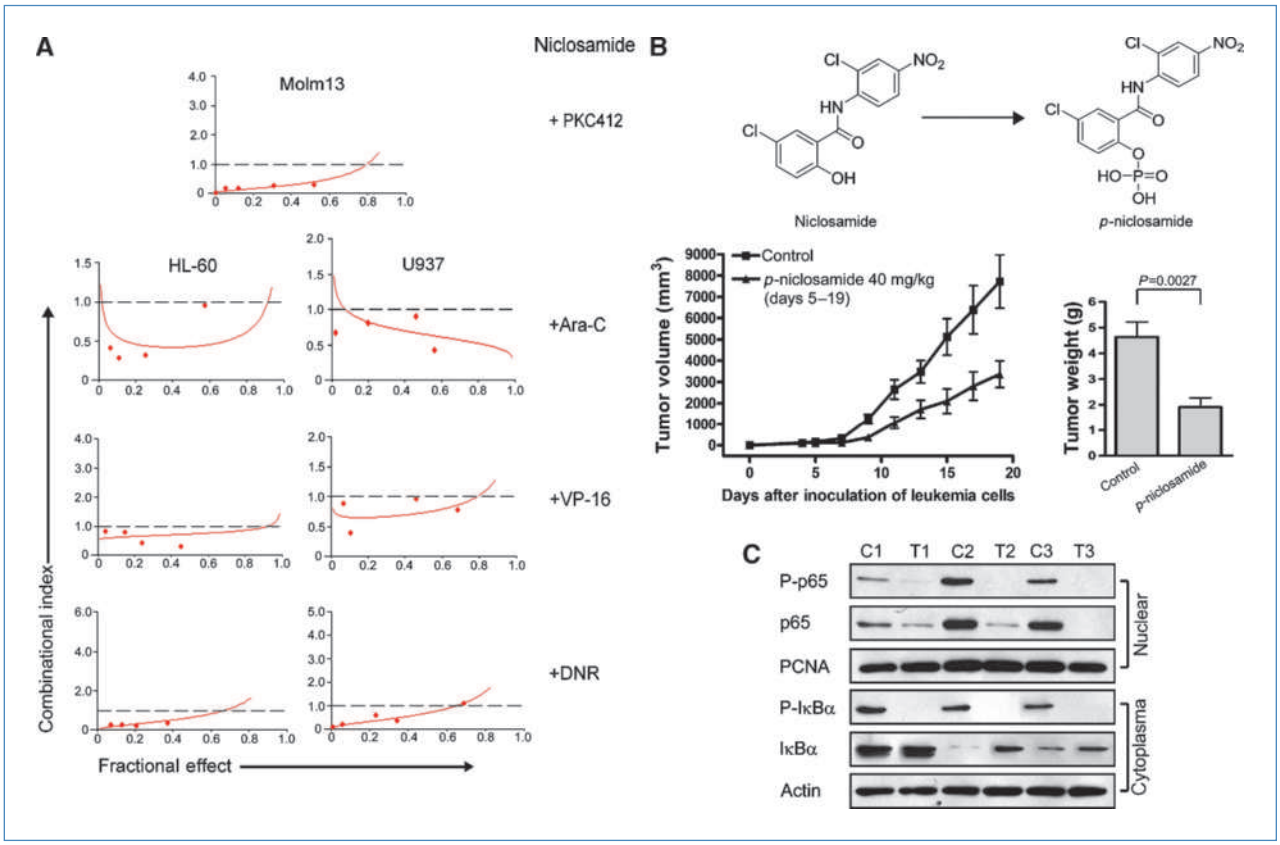

Figure 5. Niclosamide is synergistic with Ara-C, VP-16, and DNR and effective against xenografted tumor cells. A, niclosamide was synergistic with Ara-C, VP-16, and DNR and PKC412 in AML cells. B, left, nude mice bearing HL-60 xenograft tumors were treated with control (0.9% normal saline) or *p*-niclosamide (40 mg/kg/d, i.p.); right, weights of tumors dissected on day 19 after inoculation (Student's *t* test). C, immunoblotting of xenograft tissues from mice on day 19 after inoculation.

between niclosamide and PKC412 and found synergism (CI < 1) in Molm13 cells (Fig. 5A).

Niclosamide inhibits growth of xenografted AML cells in nude mice. We next explored the antineoplastic effect of niclosamide using the nude mouse xenograft model. Because niclosamide has limited solubility, we synthesized water-soluble *p*-niclosamide (Fig. 5B, top). Fourteen *nu/nu* BALB/c mice bearing HL-60 xenografts were randomized to receive treatment with normal saline (control) or *p*-niclosamide for 15 days ($n = 7$ animals each). *p*-Niclosamide (40 mg/kg/d, i.p.) potently inhibited the growth of HL-60 tumors (Fig. 5B, bottom, two-tailed Student's *t* test). Further, immunoblotting of xenograft tissues from mice revealed a potent inhibitory effect of niclosamide on the NF-κB pathway (Fig. 5C).

Niclosamide induces growth inhibition and apoptosis in primary AML cells. Our *in vitro* findings prompted us to assess the efficacy of niclosamide in primary AML cells. Niclosamide inhibited the growth of AML primary cells in a dose-dependent manner (Fig. 6A, top). The median IC_{50} value for all 81 leukemia patients (including 68 cases of AML, 10 ALL, and 3 CML) was 129 nmol/L (range, 8.5–718 nmol/L; Supplementary Table S3). Of 21 cases examined, three primary AML blast cells carrying Flt3-ITD were sensitive to niclosamide like those bearing wild-type Flt3 ($P = 0.4510$, Student's *t* test; Fig. 6A, bottom, left). As in AML cell lines, in primary AML cells, niclosamide showed a synergism with Ara-C, VP-16, and DNR (Fig. 6A, bottom, right; Supplementary Table S4). Niclosamide-treated AML blast cells from patients also showed significantly increased apoptotic cell death, as measured by flow cytometry (Fig. 6B).

Niclosamide induces apoptosis in progenitor/stem cells from AML patients. Because niclosamide could kill AML blast cells, we investigated whether it was effective in eradicating AML stem cells, which are believed to cause relapse or disease progression because of their self-renewal and proliferation capability (11, 12). First, we evaluated the effect of niclosamide on functionally defined myeloid progenitor cells by methylcellulose colony assay. The colony-forming ability was strikingly inhibited by niclosamide in a dose-dependent manner, with an IC_{50} value of 19.8 nmol/L ($n = 6$; Fig. 6C, left). In contrast, with as high as 10 μmol/L niclosamide, the number of CFU-granulocyte macrophages; burst-forming unit erythroids; and CFU-granulocytes, erythrocytes, monocytes/macrophages, and megakaryocytes in normal bone marrow cells remained ~75% that of untreated bone marrow cells ($n = 3$; Fig. 6C, right).

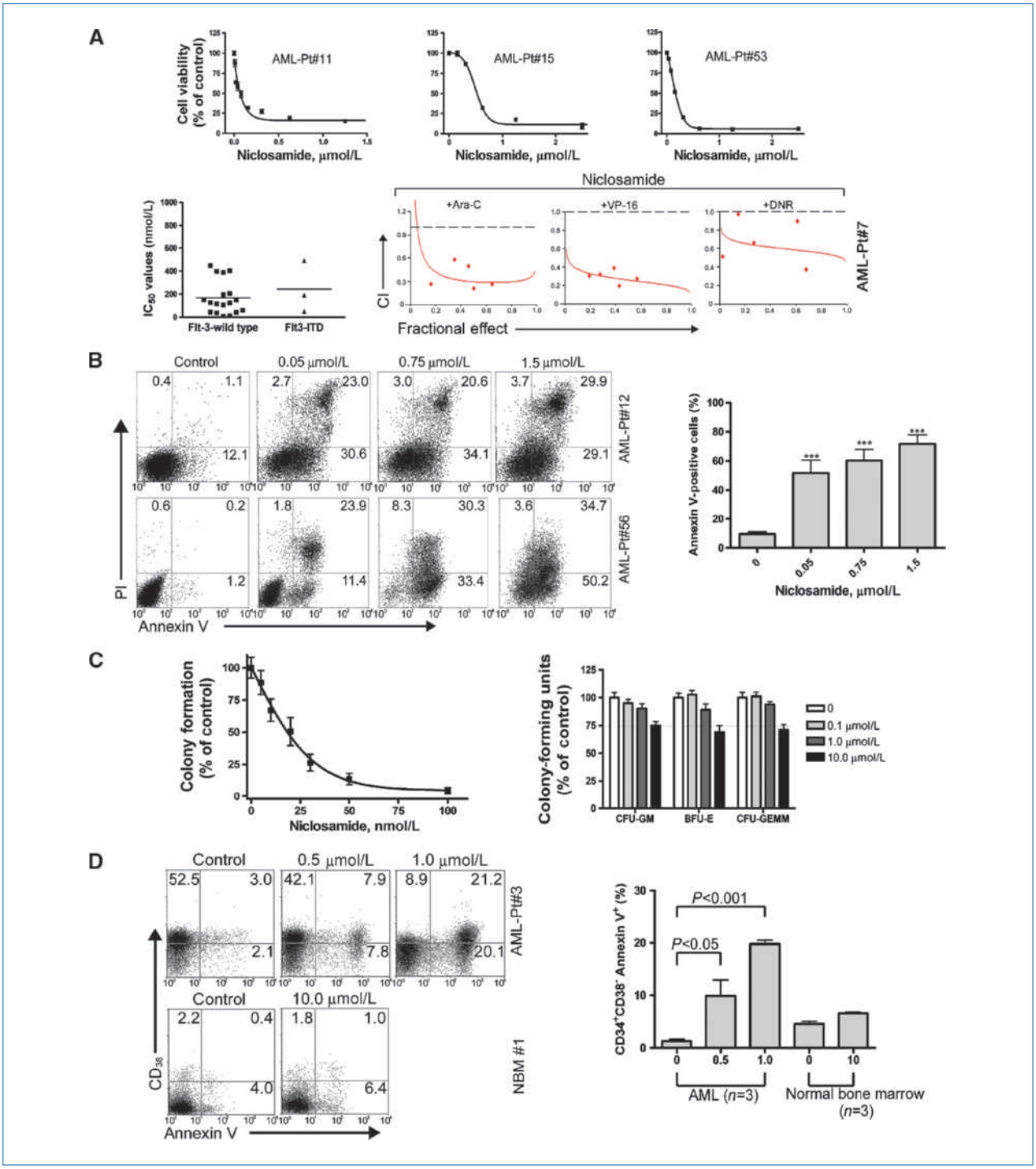

Figure 6. Effect of niclosamide on primary cells from AML patients. Primary AML blast cells from patients were treated with niclosamide for 72 h followed by MTS assay. A, top, dose-dependent curves for three representative AML patients; bottom, left, IC_{50} values of niclosamide in AML blast cells from patients with Flt3 versus Flt3-ITD; right, synergistic effect of niclosamide and the indicated drugs in AML primary blast cells. B, primary blast cells from AML patients were treated with niclosamide for 72 h; apoptosis was evaluated by flow cytometry. Left, representative histograms; right, quantitative analysis. ***, $P < 0.0001$, one-way ANOVA, post hoc comparisons, Tukey's test. $n = 10$. C, primary AML blast cells (left) or normal bone marrow cells (right) underwent methylcellulose colony assay with or without niclosamide for 10 to 14 d. CFU-GM, CFU-granulocyte macrophages; BFU-E, burst-forming unit erythroids; CFU-GEMM, CFU-granulocytes, erythrocytes, monocytes/macrophages, and megakaryocytes. D, the $CD34^+$ population separated from mononuclear cells of AML specimens (patients 3, 6, and 7) and healthy volunteers was exposed to niclosamide for 24 h and then subjected to flow cytometry after Annexin V–FITC and CD38-PE staining. *Y* axis, population of Annexin V–positive $CD34^+CD38^-$ cells by adjusting the ratio of $CD34^+$ purified cells. Representative plots are shown.

Next, we examined the effect of niclosamide on phenotypically defined stem cells from AML specimens. The $CD34^+$ population separated from mononuclear cells of AML specimens was exposed to niclosamide for 24 hours and then underwent flow cytometry with Annexin V–FITC and CD38-PE staining. Niclosamide substantially increased the Annexin V–positive $CD34^+CD38^-$ subpopulation from AML primary cells but exerted minimal effect on those from normal bone marrow (Fig. 6D). Again, the selective activity of niclosamide against AML cells versus normal bone marrow cells was confirmed in primary patient samples.

Discussion

Niclosamide is a Food and Drug Administration–approved antihelminthic active against most tapeworms. The mechanisms of its action remained elusive, although it seems to inhibit mitochondrial oxidative phosphorylation of these worms (28, 29). Niclosamide has low toxicity in mammals (oral LD_{50} in rats, >5,000 mg/kg; ref. 33) and is inexpensive and readily available. Here, we report on niclosamide as an antileukemic agent with two independent antineoplastic mechanisms: NF-κB pathway inactivation and ROS generation. We extended our work to evaluate the efficacy of niclosamide in AML and found that niclosamide potently inhibited the growth of AML cells *in vitro* and in nude mice. Niclosamide induced apoptosis selectively in AML cell lines, primary blasts, and primitive progenitor/stem cells of AML patients but not in nonmalignant cells. Niclosamide is synergistic with the frontline chemotherapeutic agents Ara-C, VP-16, and DNR. A single 5-mg/kg oral administration of niclosamide in rats could generate a maximal plasma concentration of 1.08 μmol/L (34), which is sufficient to kill AML cells, as extrapolated from our data. Our report is the first to show that niclosamide is effective *in vitro* and *in vivo* against AML cells, including those with the Flt3 mutations.

Oncogenic mutations (e.g., Flt3) can lead to constitutive activation of NF-κB (13). However, an Flt3-independent mechanism of NF-κB activation exists in some AML (13, 35). The serum level of TNFα (a well-known potent activator of NF-κB) was higher in 198 AML patients than in 48 healthy volunteers (36). The abnormal microenvironment in AML bone marrow likely causes deregulated secretion of cytokines by stromal cells (36). Therefore, inactivation of NF-κB pathway could enhance the killing effect of different chemotherapeutic agents. Indeed, our results reveal that niclosamide has synergistic effects with conventional therapeutic agents and PKC412 in AML cells.

Although niclosamide was proposed to kill parasitic helminths by uncoupling oxidative phosphorylation and disrupting $NADH \rightarrow NADP^+$ transhydrogenation (28, 29), we discovered that niclosamide causes a striking increase in ROS in human cancer cells, which at least partially contributes to the onset of apoptosis. We also showed that ROS elevation and NF-κB inactivation may be independent biological activities of niclosamide. Abrogation of ROS by NAC or deficient mitochondrial respiration did not prevent niclosamide-induced events in the NF-κB pathway; TNFα-induced activation of the NF-κB pathway did not affect ROS generation (Fig. 4D).

Notably, *p*-niclosamide showed potent antineoplastic activity against xenografted tumors in nude mice. *Ex vivo* treatment with niclosamide was effective against primary AML cells. Consistent with our findings, during the preparation of this article, Wang and colleagues (37) reported that niclosamide could kill K562 cells (CML).

Our results show that niclosamide is effective in killing AML stem cells ($CD34^+CD38^-$; Fig. 6D) but has minimal cytotoxicity against progenitor cells in normal bone marrow cells (Fig. 6C). Niclosamide may represent an important potential chemotherapeutic agent to effectively eradicate leukemia stem and progenitor cells while sparing normal hematopoietic tissue and is therefore worthy of further clinical investigation in AML.

Disclosure of Potential Conflicts of Interest

No potential conflicts of interest were disclosed.

Acknowledgments

We thank Drs. Mong-Hong Lee (M.D. Anderson Cancer Center) and Shilai Bao (Chinese Academy of Sciences) for generously providing plasmids used in this study and Dr. Peng Huang (M.D. Anderson Cancer Center) for providing C6F/HL-60 cells.

Grant Support

863 Program grant 2008AA02Z420 (J. Pan), National Natural Science Fund of China grant 90713036 (J. Pan), and 973 Program grant 2009CB825506 (J. Pan).

The costs of publication of this article were defrayed in part by the payment of page charges. This article must therefore be hereby marked *advertisement* in accordance with 18 U.S.C. Section 1734 solely to indicate this fact.

Received 10/28/2009; revised 12/08/2009; accepted 01/03/2010; published OnlineFirst 03/09/2010.

References

1. Shipley JL, Butera JN. Acute myelogenous leukemia. Exp Hematol 2009;37:649–58.
2. Stone RM, DeAngelo DJ, Klimek V, et al. Patients with acute myeloid leukemia and an activating mutation in FLT3 respond to a small-molecule FLT3 tyrosine kinase inhibitor, PKC412. Blood 2005;105:54–60.
3. Metzelder S, Wang Y, Wollmer E, et al. Compassionate use of sorafenib in FLT3-ITD-positive acute myeloid leukemia: sustained regression before and after allogeneic stem cell transplantation. Blood 2009;113:6567–71.
4. Hewamana S, Alghazal S, Lin TT, et al. The NF-κB subunit Rel A is associated with *in vitro* survival and clinical disease progression in chronic lymphocytic leukemia and represents a promising therapeutic target. Blood 2008;111:4681–9.
5. Karin M. Nuclear factor-κB in cancer development and progression. Nature 2006;441:431–6.

6. Chen F, Castranova V. Nuclear factor-κB, an unappreciated tumor suppressor. Cancer Res 2007;67:11093–8.
7. Jost PJ, Ruland J. Aberrant NF-κB signaling in lymphoma: mechanisms, consequences, and therapeutic implications. Blood 2007;109: 2700–7.
8. Frelin C, Imbert V, Griessinger E, et al. Targeting NF-κB activation via pharmacologic inhibition of IKK2-induced apoptosis of human acute myeloid leukemia cells. Blood 2005;105:804–11.
9. Carvalho G, Fabre C, Braun T, et al. Inhibition of NEMO, the regulatory subunit of the IKK complex, induces apoptosis in high-risk myelodysplastic syndrome and acute myeloid leukemia. Oncogene 2007;26:2299–307.
10. Jenkins C, Hewamana S, Gilkes A, et al. Nuclear factor-κB as a potential therapeutic target for the novel cytotoxic agent LC-1 in acute myeloid leukaemia. Br J Haematol 2008;143:661–71.
11. Guzman ML, Neering SJ, Upchurch D, et al. Nuclear factor-κB is constitutively activated in primitive human acute myelogenous leukemia cells. Blood 2001;98:2301–7.
12. Guzman ML, Rossi RM, Neelakantan S, et al. An orally bioavailable parthenolide analog selectively eradicates acute myelogenous leukemia stem and progenitor cells. Blood 2007;110:4427–35.
13. Griessinger E, Imbert V, Lagadec P, et al. AS602868, a dual inhibitor of IKK2 and FLT3 to target AML cells. Leukemia 2007;21:877–85.
14. Pelicano H, Feng L, Zhou Y, et al. Inhibition of mitochondrial respiration: a novel strategy to enhance drug-induced apoptosis in human leukemia cells by a reactive oxygen species-mediated mechanism. J Biol Chem 2003;278:37832–9.
15. Jin Y, Chen Q, Shi X, et al. Activity of triptolide against human mast cells harboring the kinase domain mutant KIT. Cancer Sci 2009;100: 1335–43.
16. Shi X, Jin Y, Cheng C, et al. Triptolide inhibits Bcr-Abl transcription and induces apoptosis in STI571-resistant chronic myelogenous leukemia cells harboring T315I mutation. Clin Cancer Res 2009;15: 1686–97.
17. Pan J, Quintas-Cardama A, Kantarjian HM, et al. EXEL-0862, a novel tyrosine kinase inhibitor, induces apoptosis *in vitro* and *ex vivo* in human mast cells expressing the KIT D816V mutation. Blood 2007; 109:315–22.
18. Sethi G, Ahn KS, Pandey MK, Aggarwal BB. Celastrol, a novel triterpene, potentiates TNF-induced apoptosis and suppresses invasion of tumor cells by inhibiting NF-κB-regulated gene products and TAK1-mediated NF-κB activation. Blood 2007;109:2727–35.
19. Ma C, Ying C, Yuan Z, et al. dp5/HRK is a c-Jun target gene and required for apoptosis induced by potassium deprivation in cerebellar granule neurons. J Biol Chem 2007;282:30901–9.
20. Shambharkar PB, Blonska M, Pappu BP, et al. Phosphorylation and ubiquitination of the IκB kinase complex by two distinct signaling pathways. EMBO J 2007;26:1794–805.
21. Blonska M, Shambharkar PB, Kobayashi M, et al. TAK1 is recruited to the tumor necrosis factor-α (TNF-α) receptor 1 complex in a receptor-interacting protein (RIP)-dependent manner and cooperates with MEKK3 leading to NF-κB activation. J Biol Chem 2005;280: 43056–63.
22. Kang MI, Henrich CJ, Bokesch HR, et al. A selective small-molecule nuclear factor-κB inhibitor from a high-throughput cell-based assay for "activator protein-1 hits". Mol Cancer Ther 2009;8:571–81.
23. Pan J, She M, Xu ZX, Sun L, Yeung SC. Farnesyltransferase inhibitors induce DNA damage via reactive oxygen species in human cancer cells. Cancer Res 2005;65:3671–81.
24. Pan J, Quintas-Cardama A, Manshouri T, et al. The novel tyrosine kinase inhibitor EXEL-0862 induces apoptosis in human FIP1L1-PDGFR-α-expressing cells through caspase-3-mediated cleavage of Mcl-1. Leukemia 2007;21:1395–404.
25. Freund D, Oswald J, Feldmann S, Ehninger G, Corbeil D, Bornhauser M. Comparative analysis of proliferative potential and clonogenicity of MACS-immunomagnetic isolated $CD34^+$ and $CD133^+$ blood stem cells derived from a single donor. Cell Prolif 2006;39:325–32.
26. Sakurai H, Miyoshi H, Toriumi W, Sugita T. Functional interactions of transforming growth factor β-activated kinase 1 with IκB kinases to stimulate NF-κB activation. J Biol Chem 1999;274:10641–8.
27. Romashkova JA, Makarov SS. NF-κB is a target of AKT in anti-apoptotic PDGF signalling. Nature 1999;401:86–90.
28. Weinbach EC, Garbus J. Mechanism of action of reagents that uncouple oxidative phosphorylation. Nature 1969;221:1016–8.
29. Park JP, Fioravanti CF. Catalysis of NADH→$NADP^+$ transhydrogenation by adult *Hymenolepis diminuta* mitochondria. Parasitol Res 2006;98:200–6.
30. Trachootham D, Alexandre J, Huang P. Targeting cancer cells by ROS-mediated mechanisms: a radical therapeutic approach? Nat Rev Drug Discov 2009;8:579–91.
31. Groeger G, Quiney C, Cotter TG. Hydrogen peroxide as a cell survival signaling molecule. Antioxid Redox Signal 2009;11:2655–71.
32. Bubici C, Papa S, Dean K, Franzoso G. Mutual cross-talk between reactive oxygen species and nuclear factor-κB: molecular basis and biological significance. Oncogene 2006;25:6731–48.
33. Merschjohann K, Steverding D. *In vitro* trypanocidal activity of the anti-helminthic drug niclosamide. Exp Parasitol 2008;118: 637–40.
34. Mercer-Haines N, Fioravanti CF. *Hymenolepis diminuta*: mitochondrial transhydrogenase as an additional site for anaerobic phosphorylation. Exp Parasitol 2008;119:24–9.
35. Birkenkamp KU, Geugien M, Schepers H, Westra J, Lemmink HH, Vellenga E. Constitutive NF-κB DNA-binding activity in AML is frequently mediated by a Ras/PI3-K/PKB-dependent pathway. Leukemia 2004;18:103–12.
36. Tsimberidou AM, Estey E, Wen S, et al. The prognostic significance of cytokine levels in newly diagnosed acute myeloid leukemia and high-risk myelodysplastic syndromes. Cancer 2008;113:1605–13.
37. Wang AM, Ku HH, Liang YC, Chen YC, Hwu YM, Yeh TS. The autonomous notch signal pathway is activated by baicalin and baicalein but is suppressed by niclosamide in K562 cells. J Cell Biochem 2009;106:682–92.